arXiv:1303.4563v1 [hep-ph] 19 Mar 2013

IPPP/13/17
DCPT/13/34
MCNET-13-03

Monte Carlo Simulation of Hard Radiation in Decays in Beyond the Standard Model Physics in Herwig++

Peter Richardson, Alexandra Wilcock

Institute of Particle Physics Phenomenology, Department of Physics
University of Durham, DH1 3LE, UK;
Email: peter.richardson@durham.ac.uk, a.h.wilcock@durham.ac.uk

Abstract

We use the POWHEG formalism in the Herwig++ event generator to match QCD real-emission matrix elements with the parton shower for a range of decays relevant to Beyond the Standard Model physics searches. Applying this correction affects the shapes of experimental observables, changing the number of events passing selection cuts. To illustrate this effect we consider the invariant-mass distribution of dijets produced in the decay of the lightest Randall-Sundrum graviton and jet measure and transverse momentum distributions for decays in Supersymmetry. We consider only the effect the POWHEG correction has on the shapes of distributions and ignore the global normalisation factor required to correct the total widths and branching ratios to next-to-leading order accuracy.

Contents

1 Introduction 2
2 POWHEG Method 3
3 Decays of BSM Particles 5
4 Results 5
5 Conclusions 9

---

1 Introduction

For Beyond the Standard Model (BSM) scenarios with additional new particles, the decays of these particles determine the experimental signals we would observe at the LHC. If the new particles have a well separated mass spectrum, long decay chains will occur when a heavy new particle is produced. For decays involving coloured particles, hard QCD radiation at each step in the decay chain will alter the structure of the event and therefore the number of events passing experimental cuts. The effects of radiation are also important in models with degenerate new particle mass spectra where decay chains are typically limited to one step. Searches for these compressed spectra scenarios look for events where hard radiation in the initial-state shower recoils against missing transverse energy in the final state to give an observable signal [1]. The emission of hard QCD radiation in the decay of new particles could either enhance or reduce this effect and so must be taken into account. Hence, accurate simulation of hard radiation in the decays of BSM particles is necessary in order to optimise searches for new physics.

Monte Carlo event generators use fixed-order matrix elements combined with parton showers and hardonization models to simulate events. In the Herwig++ event generator [2,3] the decays of unstable fundamental particles are treated separately from the hard process which produced them, prior to the parton shower phase, using the narrow width approximation. Decays are generated using the algorithm described in [4] which ensures spin correlations are correctly treated. The parton shower utilises an approximation that resums the leading collinear and leading-colour soft logarithms [5] and so does not accurately describe QCD radiation in the regions of phase space where the transverse momenta of the emitted partons are high. The Positive Weight Hardest Emission Generator (POWHEG) formalism [6] is one method that allows the simulation of high transverse momentum (hard) radiation to be improved by using the real-emission matrix element to produce the hardest emission in the shower. This approach affects both the overall cross sections for inclusive processes and results in non-global changes to the shapes of distributions sensitive to the hardest emission. In particular, non-global changes to observables such as jet transverse momenta are important since they can impact on the proportion of events passing selection cuts in new physics searches. Since BSM signals often consist of only a few events this can in turn result in significant changes to the exclusion bounds that can be set.

The POWHEG formalism has been successfully applied to a wide range of hard production processes, for example [7–27], and particle decays [28, 29] in the Standard Model (SM) as well as selected BSM processes [30–34]. Next-to-leading order (NLO) corrections to BSM particle decays have also previously been studied, for example in [35] where the super-QCD correction to the decay $\tilde{q} \to q\tilde{\chi}$ was calculated. In this work we present results from the implementation of the POWHEG method in Herwig++ for a range of decays relevant for new physics searches. A similar approach based on generic spin structures is used to apply a matrix-element correction to hard radiation in particle decays in PYTHIA [36].

The POWHEG formalism will be reviewed in Sect. 2 and in Sect. 3 details of the decay modes implemented will be given. Results for the decay of the lightest graviton in the Randall-Sundrum (RS) model [37] will be given in Sect. 4.1. Finally, results from a selection of decays in the Constrained Minimal Supersymmetric Standard Model (CMSSM) will be presented in Sect. 4.2.

2 POWHEG Method

In this section a brief outline of the POWHEG method is given. Further details can be found in [38].

In the conventional parton shower approach the inclusive differential cross section for the highest transverse momentum emission from an N body process is given by,

$$d\sigma^{\mathrm{PS}} = B(\Phi_N)d\Phi_N\left[\Delta(p_{T\mathrm{min}}) + \Delta(p_T)d\Phi_R\mathcal{P}\right]. \tag{1}$$

Here we are considering a parton shower ordered in terms of the transverse momentum of the additional parton, p_T. B is the Born-level matrix element squared including the relevant flux factor, Φ_N are the N-body phase-space variables of the leading-order (LO) process and Φ_R are the phase-space variables of the additional parton. $\mathcal{P}$ is the unregularized Altarelli-Parisi splitting kernel and $p_{T\mathrm{min}}$ is a transverse momentum cut-off introduced to regularise the infra-red (IR) divergences in the splitting function. The probability of evolving between the scales $p_{T\mathrm{max}}$ and p_T without emitting a parton is given by the Sudakov form factor

$$\Delta(p_T) = \exp\left(-\int_{p_T}^{p_{T\mathrm{max}}} d\Phi_R\mathcal{P}\,\Theta\left(p_T - p_{T\mathrm{min}}\right)\right). \tag{2}$$

The square bracket in Eq. 1 integrates to unity which ensures that the total cross section is given by the LO result.

In the POWHEG approach the inclusive differential cross section for the hardest emission is given by the QCD NLO differential cross section, that is,

$$d\sigma^{\mathrm{PO}} = \bar{B}(\Phi_N)d\Phi_N\left[\Delta^{\mathrm{PO}}(p_{T\mathrm{min}}) + \Delta^{\mathrm{PO}}(p_T)d\Phi_R\frac{R(\Phi_N,\Phi_R)}{B(\Phi_N)}\right], \tag{3}$$

where $\bar{B}(\Phi_N)$ is defined by,

$$\begin{aligned}\bar{B}(\Phi_N) = B(\Phi_N) &+ \left[V(\Phi_N) + \int C(\Phi_N,\Phi_R)d\Phi_R\right]\\ &+ \int\left[R(\Phi_N,\Phi_R)d\Phi_R - C(\Phi_N,\Phi_R)d\Phi_R\right].\end{aligned} \tag{4}$$

The real emission contribution, $R(\Phi_N, \Phi_R)$, corresponds to the radiation of an additional parton from the LO interaction and the virtual contribution, $V(\Phi_N)$, comes from the 1-loop correction to the LO process. $C(\Phi_N, \Phi_R)$ is a counter term with the same singular behaviour as the real and virtual contributions and is introduced to ensure the two square brackets in Eq. 4 are separately finite. Typically the counter term is rewritten as a sum of dipole functions, $\mathcal{D}_i$, each of which describes the singular behaviour of the matrix elements in a particular region of phase space. The Sudakov form factor appearing in Eq. 3 is,

$$\Delta^{\mathrm{PO}}(p_T) = \exp\left(-\int_{p_T}^{p_{T\max}} d\Phi_R \frac{R(\Phi_N, \Phi_R)}{B(\Phi_N)}\, \Theta\left(p_T - p_{T\min}\right)\right). \tag{5}$$

As with the conventional parton shower approach, the square bracket in Eq. 3 will integrate to unity and hence the total inclusive cross section will be given by the NLO result. The real-emission matrix element in Eq. 5 can be rewitten using dipole functions,

$$R(\Phi_N, \Phi_R) = \sum_i \frac{R(\Phi_N, \Phi_R)\mathcal{D}_i}{\sum_j \mathcal{D}_j}, \tag{6}$$

such that Eq. 5 becomes a product of Sudakov form factors, each of which describes the non-emission probability in a particular region of phase space specified by the dipole function $\mathcal{D}_i$.

When applying the POWHEG method to a parton shower ordered in transverse momentum the hardest emission is generated first using the POWHEG Sudakov form factor in Eq. 5. Subsequent emissions are generated with the normal parton shower Sudakov given in Eq. 2, with the requirement that no emissions generated using this form factor have higher transverse momentum than the hardest emission coming from $R(\Phi_N, \Phi_R)$. However in Herwig++ the shower is ordered using an angular evolution variable [2, 39] rather than the transverse momentum and as a consequence the hardest emission may not be generated first. The POWHEG approach can be reconciled with angularly ordered showers by splitting the shower into several steps [6]. First the hardest emission in the shower is generated using the POWHEG Sudakov form factor and the value of the evolution variable corresponding to this emission is determined. A truncated parton shower is then used to generate emissions for values of the evolution variable above this scale. The hardest emission is inserted and the shower is allowed to continue down to the IR cut-off of the evolution variable. Finally, any emissions generated by the shower that are harder than the one generated using the POWHEG Sudakov form factor are vetoed.

3 Decays of BSM Particles

As discussed in Sect. 1, it is important that the simulation of QCD radiation in the decays of BSM particles is done in the most accurate way possible. In this work we present results illustrating the effect of consistently matching the QCD real-emission matrix element with the parton shower in Herwig++ through the POWHEG formalism. This technique has been applied to a range of decays that occur in most of the well studied BSM scenarios. Table 1 shows the combinations of incoming and outgoing spins for which this method is used and each spin structure is implemented for the colour flows given in Table 2. However, models with coloured tensor particles are beyond the scope of this work and therefore decays involving incoming tensor particles were limited to colour flows in which the tensor is a colour singlet.

The LO and real-emission matrix elements appearing in the POWHEG Sudakov form factor in Eq. 5 are calculated using helicity amplitude methods to correctly incorporate spin correlations [4]. The dipole functions, $\mathcal{D}_i$, that appear in Eq. 6 are defined as in the Catani-Seymour dipole subtraction method [40,41]. In this approach dipoles describing quasi-collinear radiation from massive vector bosons are not well defined. Hence the Fermion-Fermion-Vector, Scalar-Scalar-Vector and Tensor-Vector-Vector decays are limited to the situation where any final-state coloured vector particles are massless. The Vector-Fermion-Fermion and Vector-Scalar-Scalar decays do however include radiation from massive incoming vector particles. Decays are performed in the rest frame of the decaying particle [2] and therefore the dipole describing the singular behaviour of this particle will only contain a universal soft contribution. This is a well defined, spin-independent function.

Finally, in this work we focus solely on the effect of the POWHEG correction on the shapes of observable distributions and have not implemented the global normalisation factor coming from the presence of $\bar{B}$ rather than B in Eq. 3. In most cases the partial widths and branching ratios used in Herwig++ are calculated by an external program and so the implementation of the $\bar{B}$ function will not affect the results. Even in cases where the calculation of the widths and branching ratios is performed in Herwig++ the impact of the POWHEG correction on the real radiation will be the dominant effect.

4 Results

4.1 Randall-Sundrum Graviton

The effect of applying the POWHEG correction to the decay of the lightest RS graviton was investigated using the Herwig++ implementation of the RS model. LHC proton-proton collisions with a centre-of-mass (CM) energy of $\sqrt{s} = 8\,\mathrm{TeV}$ were simulated. The lightest graviton, G, was produced as a resonance and

Incoming	**Outgoing**
Scalar	Scalar Scalar
Scalar	Scalar Vector
Scalar	Fermion Fermion
Fermion	Fermion Scalar
Fermion	Fermion Vector
Vector	Scalar Scalar
Vector	Fermion Fermion
Tensor	Fermion Fermion
Tensor	Vector Vector

Tab. 1: Spin combinations for which the POWHEG correction has been applied.

Incoming	**Outgoing**
0	$3\ \bar{3}$
0	$8\ 8$
3	$3\ 0$
$\bar{3}$	$\bar{3}\ 0$
3	$3\ 8$
$\bar{3}$	$\bar{3}\ 8$
8	$3\ \bar{3}$

Tab. 2: Colour flows for which the POWHEG correction has been applied.

allowed to decay via $G \to gg$ and $G \to q\bar{q}$ for $q = u, d, s, c, b$. The mass of the graviton was chosen to be $m_G = 2.23\,\text{TeV}$ which corresponds to the lower bound on the allowed graviton mass for the coupling $k/\bar{M}_{pl} = 0.1$ in [42]. An analysis based on the ATLAS experiment's search for new phenomena in dijet distributions [43] was then carried out. Jets were constructed using the FastJet [44] implementation of the anti-k_t algorithm [45] with the energy recombination scheme and a distance parameter $R = 0.6$. Jets with $|y| \geq 4.4$ were discarded, where y is the rapidity of the jet in the pp CM frame. Events with less than two jets passing this constraint were vetoed. The rapidities of the two highest p_T jets in the pp CM frame are given by y_1 and y_2. In the dijet CM frame formed by the two hardest jets their corresponding rapidities are y_* and $-y_*$ where $y_* = \frac{1}{2}(y_1 - y_2)$. Events not satisfying $|y_*| < 0.6$ and $|y_{1,2}| < 2.8$ were discarded. The dijet invariant mass, m_{jj}, was formed from the vector sum of the two hardest jet momenta and events were vetoed if $m_{jj} \leq 1.0\,\text{TeV}$.

The dijet mass distribution after the above selection cuts were applied is shown in the left hand plot in Fig. 1. The blue dashed line shows the invariant mass distribution for the LO matrix element combined with the parton shower while the black line shows the result with the POWHEG correction to the graviton decay applied. Including the POWHEG correction causes a significant decrease in the number of events in the region $2.1\,\text{TeV} \leq m_{jj} \leq 2.3\,\text{TeV}$. This effect is highlighted in the right hand plot in Fig. 1 which shows the dijet mass distribution in this range. The number of events in this region decreases by approximately a factor of 1.6 when the POWHEG correction is applied. Of the 10^7 events generated 2.4% pass the event selection cuts for the standard parton shower approach whereas only 1.5% pass when the POWHEG correction is applied. In the conventional parton shower approach, the majority of the graviton's momentum will be carried by the two partonic decay products. When the POWHEG correction

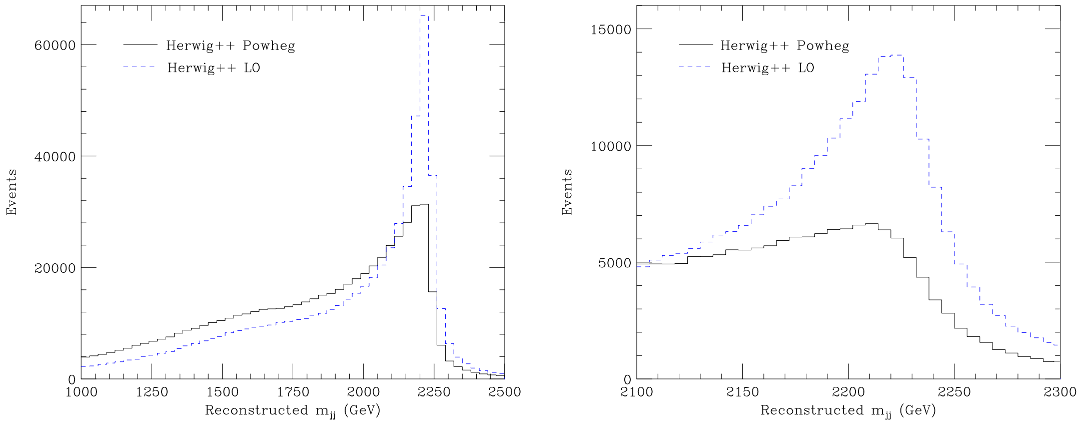

Fig. 1: Dijet invariant mass distribution for the lightest RS graviton decaying to jets. The left-hand plot shows the distribution in the full range $1.0\,\text{TeV} \leq m_{jj} \leq 2.5\,\text{TeV}$ while the right-hand plot emphasises the effect on the peak region $2.1\,\text{TeV} \leq m_{jj} \leq 2.3\,\text{TeV}$. The mass of the graviton was $m_G = 2.23\,\text{TeV}$ and the coupling $k/\bar{M}_{pl} = 0.1$. LHC events were simulated with $\sqrt{s} = 8\,\text{TeV}$.

is applied, the highest p_T emission in the shower will typically be quite hard and so a significant fraction of the the graviton's momentum will be missed by considering the invariant mass of only the hardest two jets, therefore shifting the distribution to lower values of m_{jj}.

4.2 Constrained Minimal Supersymmetric Standard Model

In addition to the results presented in Sect. 4.1 the effect of the POWHEG correction was also studied in the context of the CMSSM model. The high scale parameters of the model were chosen to be $m_0 = 1460\,\text{GeV}$, $m_{1/2} = 600\,\text{GeV}$, $\tan\beta = 10$, $A_0 = 0$ and $\mu > 0$. This point lies just outside the exclusion limits set by the ATLAS experiment in [46]. The corresponding weak scale parameters and decay modes were calculated using ISAJET 7.80 [47]. The **Herwig++** implementation of the MSSM model was used to generate LHC pp collisions at a centre-of-mass energy of $\sqrt{s} = 8\,\text{TeV}$. In the following sections the impact of the POWHEG correction on a number of archetypal decays is presented.

4.2.1 $\tilde{u}_L \to u\,\tilde{\chi}_1^0$

Events were generated in which $\tilde{u}_L$ and its associated anti-particle were produced and then decayed via the mode $\tilde{u}_L \to u\,\tilde{\chi}_1^0$. The final-state particles from each decay, excluding the $\tilde{\chi}_1^0$, were clustered into jets using the **FastJet** implementation of the anti-k_T algorithm with the energy recombination scheme and $R = 0.4$.

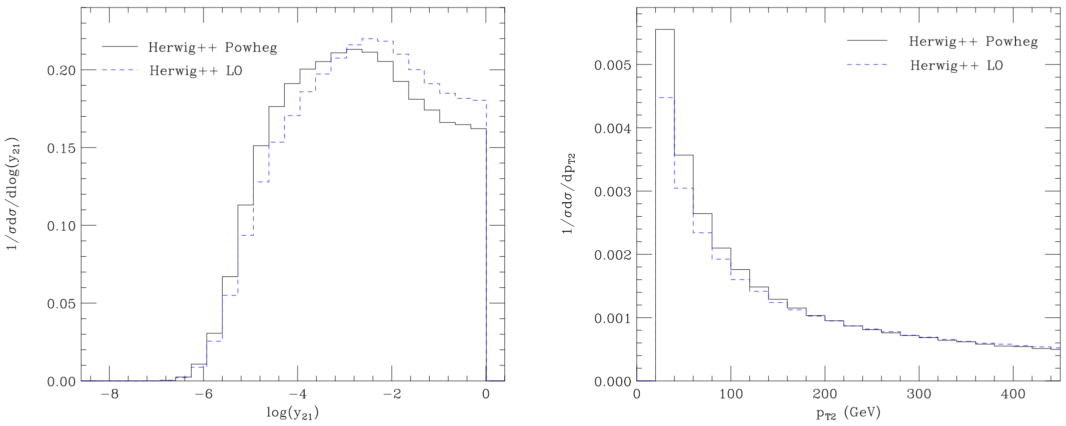

Fig. 2: Comparison of distributions generated with and without the POWHEG correction for the decay $\tilde{u}_L \rightarrow u\,\tilde{\chi}^0_1$ in the CMSSM model with $m_0 = 1460\,\mathrm{GeV}$, $m_{1/2} = 600\,\mathrm{GeV}$, $\tan\beta = 10$, $A_0 = 0$ and $\mu > 0$ at the LHC with $\sqrt{s} = 8\,\mathrm{TeV}$. The left-hand plot shows the logarithm of the jet measure y_{21} and the right-hand plot the p_T of the the second hardest jet in the decay, both in the rest frame of the $\tilde{u}_L$.

Jets with $p_T \leq 20\,\mathrm{GeV}$ or $|\eta| > 2.8$ were discarded. The jet measure y_{21}, as defined in [48], was calculated in the rest frame of the decaying $\tilde{u}_L$ and the corresponding distribution of $\log y_{21}$ is shown in the left-hand plot in Fig. 2. The right-hand plot in Fig. 2 shows the transverse momentum distribution of the second hardest jet in the decay. In both plots the blue dashed line corresponds to the distribution generated using the LO matrix element combined with the parton shower while the black solid line shows the result with the POWHEG correction to the decay applied. Including the POWHEG correction has the effect of shifting the distribution in the left-hand plot of Fig. 2 to lower values of the jet measure. This happens because the parton shower in Herwig++ tends to over-populate the hard region of phase space. With the POWHEG correction applied, the hardest emission in the shower is now correctly generated using the real-emission matrix element and hence the over population is reduced. The same effect can be seen in the p_{T2} distribution in the right hand plot of Fig. 2.

4.2.2 $\tilde{u}_L \rightarrow u\,\tilde{g}$

The scenario where $\tilde{u}_L$ decays through the mode $\tilde{u}_L \rightarrow u\,\tilde{g}$ was also studied. To focus on the impact of the POWHEG correction to this decay the gluinos produced were not allowed to decay further. Events were generated at the parton level to accommodate the production of stable gluinos and were analysed as in Sect. 4.2.1. Distributions of $\log y_{32}$ and p_{T3} in the rest frame of the $\tilde{u}_L$ were plotted and are shown in the left and right hand plots of Fig. 3 respectively.

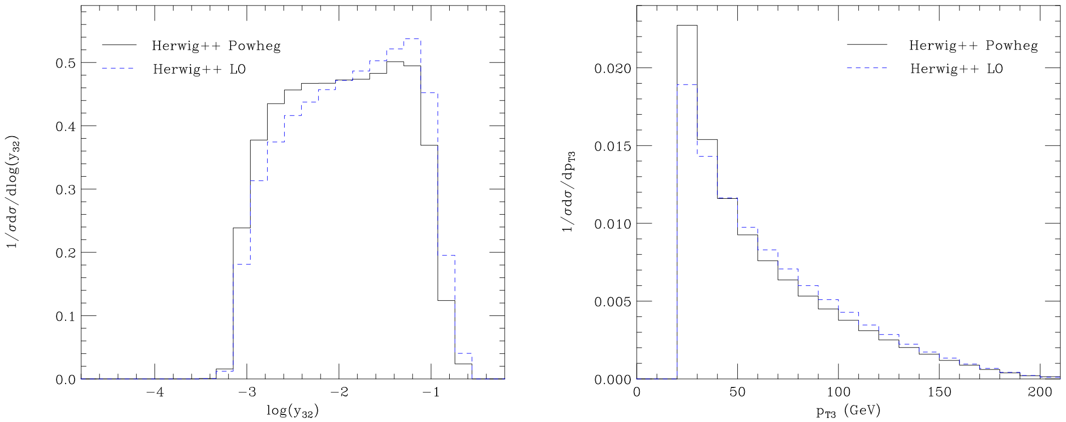

Fig. 3: Comparison of distributions generated with and without the POWHEG correction applied to the decay $\tilde{u}_L \to u\,\tilde{g}$ for stable gluinos. Results are for the CMSSM model with $m_0 = 1460\,\mathrm{GeV}$, $m_{1/2} = 600\,\mathrm{GeV}$, $\tan\beta = 10$, $A_0 = 0$ and $\mu > 0$ for LHC events with $\sqrt{s} = 8\,\mathrm{TeV}$. The left-hand plot shows the logarithm of the jet measure y_{32} and the right-hand plot the p_T of the the third hardest jet in the decay, both in the rest frame of the $\tilde{u}_L$.

The blue dashed line shows the purely LO result and the black solid line is the result including the POWHEG correction. As in Sect. 4.2.1, we find that the POWHEG correction reduces the p_T of the third hardest jet and shifts the jet measure distribution to lower values of $\log y_{32}$.

4.2.3 $\tilde{b}_2 \to W^- \tilde{t}_1$

Finally, events were simulated where the heavier superpartner of the bottom quark, $\tilde{b}_2$, was pair produced and decayed via $\tilde{b}_2 \to W^- \tilde{t}_1$. Parton level events were generated with stable $\tilde{t}_1$ and leptonically decaying W bosons. The final state particles were analysed as in Sect. 4.2.1 with the decay products of the W bosons omitted from the jet clustering. Distributions of $\log y_{21}$ and p_{T2} were plotted and are shown in Fig. 4. As in Sect. 4.2.1 and 4.2.2 we see that the POWHEG correction softens the $\log y_{21}$ and p_{T2} distributions.

5 Conclusions

In this work we used the real-emission matrix element to generate hard QCD radiation in a range of particle decays in the Herwig++ event generator. This method is particularly relevant to new physics searches based on the decays of heavy new particles produced in LHC collisions. The POWHEG corrections to these decays can change the shapes of certain experimental observables, thus

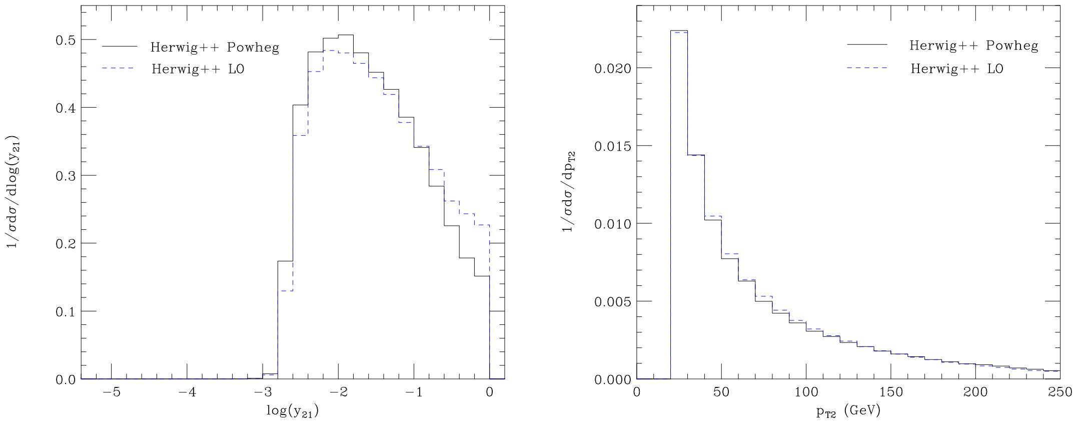

Fig. 4: Comparison of distributions generated with and without the POWHEG correction applied to the decay $\tilde{b}_2 \to W^- \tilde{t}_1$ for stable $\tilde{t}_1$ and leptonically decaying W bosons. Results are for the CMSSM model with $m_0 = 1460\,\mathrm{GeV}$, $m_{1/2} = 600\,\mathrm{GeV}$, $\tan\beta = 10$, $A_0 = 0$ and $\mu > 0$ at the LHC with $\sqrt{s} = 8\,\mathrm{TeV}$. The left-hand plot shows the logarithm of the jet measure y_{21} and the right-hand plot the p_T of the the second hardest jet in the decay, both in the rest frame of the $\tilde{b}_2$.

altering the number of signal events passing selection cuts and modifying the exclusion bounds that can be set on the masses of the new particles. This correction will be available in a future version of Herwig++ .

The technique was tested by plotting the invariant mass distribution of dijets produced in the decay of the lightest RS graviton, $G \to gg$ and $G \to q\bar{q}$. Applying the POWHEG correction was found to have a considerable impact on the height of the distribution in the dijet mass peak. The percentage of events passing selection cuts in the mass range $2.1\,\mathrm{TeV} \leq m_{jj} \leq 2.3\,\mathrm{TeV}$ dropped from 2.4% to 1.5% when the correction was applied. This corresponds to a decrease by a factor of approximately 1.6. This is a consequence of the dijet invariant mass not including the hardest emission in the shower that will carry a significant fraction of the graviton's momentum when it is simulated using the real-emission matrix element. This illustrates the importance of including higher order corrections when optimising experimental searches.

The POWHEG correction was also tested for a range of decays in the CMSSM model. Here it was found that the correction reduced the transverse momentum of the hardest emission in the decay. This leads to a softening of the p_T and jet measure distributions.

In this work we have used the POWHEG formalism to improve the simulation of hard radiation in particle decays and studied the resulting effect on experimental observables. However, hard radiation in the initial-state parton shower can also have a significant impact on these distributions. Hence, in order to achieve accurate simulation of hard radiation in BSM processes we must also include effects from the initial-state shower. Using the POWHEG formalism to improve the simulation of the hardest initial-state emission in the shower will be the subject of future work.

6 Acknowledgements

We are grateful for help from the other members of the Herwig++ collaboration. This work was supported by the Science and Technology Facilities Council. We also acknowledge the support of the European Union via MCNet.

References

[1] J. F. Gunion and S. Mrenna, *A Study of SUSY signatures at the Tevatron in models with near mass degeneracy of the lightest chargino and neutralino*, *Phys.Rev.* **D62** (2000) 015002, [`hep-ph/9906270`].

[2] M. Bahr, S. Gieseke, M. Gigg, D. Grellscheid, K. Hamilton, et al., *Herwig++ Physics and Manual*, *Eur.Phys.J.* **C58** (2008) 639–707, [`arXiv:0803.0883`]. 143 pages, program and additional information available from http://projects.hepforge.org/herwig.

[3] K. Arnold, L. d'Errico, S. Gieseke, D. Grellscheid, K. Hamilton, et al., *Herwig++ 2.6 Release Note*, `arXiv:1205.4902`.

[4] P. Richardson, *Spin correlations in Monte Carlo simulations*, *JHEP* **0111** (2001) 029, [`hep-ph/0110108`].

[5] A. Buckley, J. Butterworth, S. Gieseke, D. Grellscheid, S. Hoche, et al., *General-purpose event generators for LHC physics*, *Phys.Rept.* **504** (2011) 145–233, [`arXiv:1101.2599`].

[6] P. Nason, *A New method for combining NLO QCD with shower Monte Carlo algorithms*, *JHEP* **0411** (2004) 040, [`hep-ph/0409146`].

[7] S. Frixione, P. Nason, and G. Ridolfi, *A Positive-weight next-to-leading-order Monte Carlo for heavy flavour hadroproduction*, *JHEP* **0709** (2007) 126, [`arXiv:0707.3088`].

[8] S. Alioli, P. Nason, C. Oleari, and E. Re, *NLO vector-boson production matched with shower in POWHEG*, *JHEP* **0807** (2008) 060, [`arXiv:0805.4802`].

[9] K. Hamilton, P. Richardson, and J. Tully, *A Positive-Weight Next-to-Leading Order Monte Carlo Simulation of Drell-Yan Vector Boson Production*, *JHEP* **0810** (2008) 015, [`arXiv:0806.0290`].

[10] S. Alioli, P. Nason, C. Oleari, and E. Re, *NLO Higgs boson production via gluon fusion matched with shower in POWHEG*, *JHEP* **0904** (2009) 002, [`arXiv:0812.0578`].

[11] P. Nason and C. Oleari, *NLO Higgs boson production via vector-boson fusion matched with shower in POWHEG*, *JHEP* **1002** (2010) 037, [`arXiv:0911.5299`].

[12] S. Alioli, P. Nason, C. Oleari, and E. Re, *NLO single-top production matched with shower in POWHEG: s- and t-channel contributions*, *JHEP* **0909** (2009) 111, [`arXiv:0907.4076`].

[13] K. Hamilton, P. Richardson, and J. Tully, *A Positive-Weight Next-to-Leading Order Monte Carlo Simulation for Higgs Boson Production*, *JHEP* **0904** (2009) 116, [`arXiv:0903.4345`].

[14] E. Re, *Single-top Wt-channel production matched with parton showers using the POWHEG method*, *Eur.Phys.J.* **C71** (2011) 1547, [`arXiv:1009.2450`].

[15] K. Hamilton, *A positive-weight next-to-leading order simulation of weak boson pair production*, *JHEP* **1101** (2011) 009, [`arXiv:1009.5391`].

[16] S. Alioli, P. Nason, C. Oleari, and E. Re, *Vector boson plus one jet production in POWHEG*, *JHEP* **1101** (2011) 095, [`arXiv:1009.5594`].

[17] S. Alioli, K. Hamilton, P. Nason, C. Oleari, and E. Re, *Jet pair production in POWHEG*, *JHEP* **1104** (2011) 081, [`arXiv:1012.3380`].

[18] S. Platzer and S. Gieseke, *Dipole Showers and Automated NLO Matching in Herwig++*, *Eur.Phys.J.* **C72** (2012) 2187, [`arXiv:1109.6256`].

[19] C. Oleari and L. Reina, *W +- b $\bar{b}$ production in POWHEG*, *JHEP* **1108** (2011) 061, [`arXiv:1105.4488`].

[20] T. Melia, P. Nason, R. Rontsch, and G. Zanderighi, *W^+W^+ plus dijet production in the POWHEGBOX*, *Eur.Phys.J.* **C71** (2011) 1670, [`arXiv:1102.4846`].

[21] B. Jager and G. Zanderighi, *NLO corrections to electroweak and QCD production of W+W+ plus two jets in the POWHEGBOX*, *JHEP* **1111** (2011) 055, [`arXiv:1108.0864`].

[22] T. Melia, P. Nason, R. Rontsch, and G. Zanderighi, *W+W-, WZ and ZZ production in the POWHEG BOX*, *JHEP* **1111** (2011) 078, [`arXiv:1107.5051`].

[23] L. D'Errico and P. Richardson, *Next-to-Leading-Order Monte Carlo Simulation of Diphoton Production in Hadronic Collisions*, *JHEP* **1202** (2012) 130, [`arXiv:1106.3939`].

[24] L. D'Errico and P. Richardson, *A Positive-Weight Next-to-Leading-Order Monte Carlo Simulation of Deep Inelastic Scattering and Higgs Boson Production via Vector Boson Fusion in Herwig++*, *Eur.Phys.J.* **C72** (2012) 2042, [`arXiv:1106.2983`].

[25] B. Jager, S. Schneider, G. Zanderighi, S. Schneider, and G. Zanderighi, *Next-to-leading order QCD corrections to electroweak Zjj production in the POWHEGBOX*, *JHEP* **1209** (2012) 083, [`arXiv:1207.2626`].

[26] E. Re, *NLO corrections merged with parton showers for Z+2 jets production using the POWHEG method*, *JHEP* **1210** (2012) 031, [`arXiv:1204.5433`].

[27] B. Jager and G. Zanderighi, *Electroweak W+W-jj prodution at NLO in QCD matched with parton shower in the POWHEG-BOX*, `arXiv:1301.1695`.

[28] O. Latunde-Dada, *Applying the POWHEG method to top pair production and decays at the ILC*, *Eur.Phys.J.* **C58** (2008) 543–554, [`arXiv:0806.4560`].

[29] P. Richardson and D. Winn, *Investigation of Monte Carlo Uncertainties on Higgs Boson searches using Jet Substructure*, *Eur.Phys.J.* **C72** (2012) 2178, [`arXiv:1207.0380`].

[30] A. Papaefstathiou and O. Latunde-Dada, *NLO production of W ’ bosons at hadron colliders using the MC@NLO and POWHEG methods*, *JHEP* **0907** (2009) 044, [`arXiv:0901.3685`].

[31] E. Bagnaschi, G. Degrassi, P. Slavich, and A. Vicini, *Higgs production via gluon fusion in the POWHEG approach in the SM and in the MSSM*, *JHEP* **1202** (2012) 088, [`arXiv:1111.2854`].

[32] M. Klasen, K. Kovarik, P. Nason, and C. Weydert, *Associated production of charged Higgs bosons and top quarks with POWHEG*, *Eur.Phys.J.* **C72** (2012) 2088, [`arXiv:1203.1341`].

[33] I. Fridman-Rojas and P. Richardson, *Next-to-Leading Order Simulation of Slepton Pair Production*, `arXiv:1208.0279`.

[34] B. Jager, A. von Manteuffel, and S. Thier, *Slepton pair production in the POWHEG BOX*, *JHEP* **1210** (2012) 130, [`arXiv:1208.2953`].

[35] R. Horsky, . Kramer, Michael, A. Muck, and P. M. Zerwas, *Squark Cascade Decays to Charginos/Neutralinos: Gluon Radiation*, *Phys.Rev.* **D78** (2008) 035004, [`arXiv:0803.2603`].

[36] E. Norrbin and T. Sjostrand, *QCD radiation off heavy particles*, *Nucl.Phys.* **B603** (2001) 297–342, [`hep-ph/0010012`].

[37] L. Randall and R. Sundrum, *A Large mass hierarchy from a small extra dimension*, *Phys.Rev.Lett.* **83** (1999) 3370–3373, [`hep-ph/9905221`].

[38] S. Frixione, P. Nason, and C. Oleari, *Matching NLO QCD computations with Parton Shower simulations: the POWHEG method*, *JHEP* **0711** (2007) 070, [`arXiv:0709.2092`].

[39] S. Gieseke, P. Stephens, and B. Webber, *New formalism for QCD parton showers*, *JHEP* **0312** (2003) 045, [`hep-ph/0310083`].

[40] S. Catani and M. Seymour, *A General algorithm for calculating jet cross-sections in NLO QCD*, *Nucl.Phys.* **B485** (1997) 291–419, [`hep-ph/9605323`].

[41] S. Catani, S. Dittmaier, M. H. Seymour, and Z. Trocsanyi, *The Dipole formalism for next-to-leading order QCD calculations with massive partons*, *Nucl.Phys.* **B627** (2002) 189–265, [`hep-ph/0201036`].

[42] **ATLAS Collaboration** Collaboration, G. Aad et al., *Search for Extra Dimensions in diphoton events using proton-proton collisions recorded at* $\sqrt{s} = 7$ *TeV with the ATLAS detector at the LHC*, `arXiv:1210.8389`.

[43] **ATLAS Collaboration** Collaboration, G. Aad et al., *ATLAS search for new phenomena in dijet mass and angular distributions using pp collisions at* $\sqrt{s} = 7$ *TeV*, `arXiv:1210.1718`.

[44] M. Cacciari, G. P. Salam, and G. Soyez, *FastJet User Manual*, *Eur.Phys.J.* **C72** (2012) 1896, [`arXiv:1111.6097`].

[45] M. Cacciari, G. P. Salam, and G. Soyez, *The Anti-k(t) jet clustering algorithm*, *JHEP* **0804** (2008) 063, [`arXiv:0802.1189`].

[46] **ATLAS Collaboration** Collaboration, *Search for squarks and gluinos with the ATLAS detector using final states with jets and missing transverse momentum and 5.8 fb*$^{-1}$ *of* $\sqrt{s}$*=8 TeV proton-proton collision data*, .

[47] F. E. Paige, S. D. Protopopescu, H. Baer, and X. Tata, *ISAJET 7.69: A Monte Carlo event generator for pp, anti-p p, and e+e- reactions*, `hep-ph/0312045`.

[48] **ATLAS Collaboration** Collaboration, G. Aad et al., *Measurement of event shapes at large momentum transfer with the ATLAS detector in pp collisions at* $\sqrt{s} = 7$ *TeV*, *Eur.Phys.J.* **C72** (2012) 2211, [`arXiv:1206.2135`].